4PoA04 IEEE Trans. Appl. Supercond.

Characterization of Japan's DEMO Candidate Reinforced Nb_3Sn Wires under Crossover Contact Stress

Nobuya Banno, Toshihisa Asano, Tsuyoshi Yagai, Shinya Kawashima, Masahiro Sugimoto, Satoshi Awaji, Hiroyasu Utoh, and Yoshiteru Sakamoto

***Abstract*— The size of Japan's demonstration power plant (JA DEMO) reactor is planned to be approximately 1.4 times larger than that of ITER magnet. Mechanical behavior and the reinforcement of the Nb_3Sn strands under a complex distribution of electromagnetic force in the cable-in-conduit conductor (CICC) are of great concern. In this study, an experimental setup for I_c measurement under crossover contact stress in external magnetic fields, which is regarded as more realistic situation in CICC, was constructed. Then, we studied superconducting properties and microstructures of JA DEMO candidate reinforced Nb_3Sn wires under crossover contact stress. CuNb-reinforced bronze-route Nb_3Sn wires made by Furukawa Electric and distributed-tin (DT) Nb_3Sn wires reinforced with brass matrix made by Kobe Steel were tested. The reinforced wires have shown better I_c properties against contact stress, compared with conventional Cu matrix wires. Under contact stress, the outer copper sheath was predominantly deformed, which is believed to contribute to relaxation of the stress concentration. The brass matrix seems to be significantly effective in suppressing distortion in the filament region. The use of reinforced Nb_3Sn wires increases the reliability of the TF magnet operation.**

***Index Terms*— Crossover contact stress, DEMO, Nb_3Sn, Reinforcement**

I. INTRODUCTION

THE Joint Special Design Team for Fusion DEMO [1] is conducting the conceptual designing of Japan's fusion demonstration (JA DEMO) reactor, whose size is planned to be approximately 1.4 times larger than the ITER magnet [2], [3]. Increase in the toroidal magnetic field (TF) and the operation current forces the conductor in the TF coil to undergo approximately 1.5 times higher electromagnetic force than that of the ITER TF [4], [5]. Short twist pitch designs for CICC are expected to suppress severe damage in the brittle Nb_3Sn strands due to the buckling of the strands [6]–[13]. Therefore, the JA DEMO design team is currently considering the adoption of a short twist pitch design for every cabling stage of the CICC.

However, the huge transverse electromagnetic force in TF coil still remains even in the short twist pitch design. The hoop stress by the electromagnetic force releases slightly the axial compressive stress of the cable, that is caused by a thermal contraction of the stainless-steel conduit, while the majority of the electromagnetic force is expected to be applied to the cable in the conduit in the radial direction of the TF coil. Using the designed cable diameter of 50.4 mm for DEMO TF CICC, the average electromagnetic force is calculated to be approximately 23 MPa. This value itself is not so high. However, considering the fact that twisted strands make point contact with each other, very high stresses are concerned to be locally applied to the strands. Furthermore, there are also manufacturing problems with short-pitch cabling such as strand buckling and breakage [14]. This may demand a longer twist pitch in the cable, resulting in increase in the effective strain of the cable in operations. Hence, strengthening the Nb_3Sn strands are highly required to ensure the high performance of CICC.

Against this background, we have previously investigated the microstructure and superconducting properties under bending strain for JA DEMO candidate reinforced Nb_3Sn strands [15]: the distributed-tin (DT) strand reinforced with a brass matrix (made by Kobe Steel, Ltd.) [16] and the CuNb reinforced bronze-route Nb_3Sn strand (made by Furukawa Electric Co., Ltd.) [17], [18]. The previous results obtained through scanning electron microscopy (SEM)-electron backscatter diffraction (EBSD) analysis and cryogenic current test have revealed that the reinforcement for the matrix and outer sheath is effective for improving stress tolerance against bending.

In this study, the superconducting properties and microstructure of the JA DEMO candidate reinforced Nb_3Sn wires were evaluated under crossover contact stress as more realistic situation in CICC. An experimental setup for critical

Submitted for review September 19, 2023

This work was supported by QST Research Collaboration for Fusion DEMO (04K067). *(Corresponding author: Nobuya Banno.)*

N. Banno is with the Research Center for Energy and Environmental Materials, National Institute for Materials Science, Tsukuba, Ibaraki 305-0047, Japan (e-mail: banno.nobuya@nims.go.jp).

T. Asano is with National Institute for Materials Science, Tsukuba, Ibaraki 305-0047, Japan.

T. Yagai is with Sophia University, Tokyo 102-8554, Japan.

Shinya Kawashima is with Kobe Steel Ltd., Kobe 651-2271, Japan.

M. Sugimoto is with Furukawa Electric Co., Ltd., Tochigi 321-1493, Japan.

S. Awaji is with the High Field Laboratory for Superconducting Materials, Institute for Material Research, Tohoku University, Sendai 980-8577, Japan.

H. Utoh, and Y. Sakamoto are with the Rokkasho Fusion Institute, National Institutes for Quantum Science and Technology, Rokkasho, Aomori 039-3212, Japan.

Color versions of one or more of the figures in this paper are available online at http://ieeexplore.ieee.org.

Digital Object Identifier will be inserted here upon acceptance.

current (I_c) measurement was newly developed. The SEM-EBSD strain analysis for residual strain after loading indicated that the outer Cu sheath is predominantly deformed, resulting in relaxation of the stress concentration to the filamentary region. The reinforced strands exhibited better I_c characteristics under contact stress than that of the normal Cu matrix wire. Notably, stress sensitivity of the brass-matrix DT wires was substantially small, compared with conventional Cu-matrix DT wires.

II. Experimental

A. Setup for I_c measurement

Fig. 1 illustrates schematically crossover contact between strands in CICC under the electromagnetic force, and the developed setup for I_c measurement simulating crossover contact stress state. During the compaction of the conduit with the twisted cable inside, the strands are optimally rearranged, and some strands should ride up on top of others. Although many measurement systems under transverse load have been demonstrated [19]–[25], the I_c measurement system under crossover contact stress was chosen here because it is believed to be more realistic situation for strands subjected to a transverse electromagnetic force in the CICC.

The design and configuration of the setup was determined through lots of trial and error. The wire sample with a length of 37 mm is soldered at both ends to the electrodes over a distance of 11 mm. The voltage tap distance was 10 mm. Then, the dummy same wire is placed on the top of the sample orthogonally to the sample. The electrodes are screwed to the current leads. Great care was taken in mounting the sample on the probe not to damage the sample.

A transverse load is applied by a stepping motor and the load value is measured by a load cell that is available in a 50 kg capacity. The fixed anvil is made of stainless-steel, which is placed on the GFRP table. The load is transmitted to the wire through the GFRP anvil with a diameter of 5 mm. A displacement gauge is set to measure the total displacement including the sample deformation, an elongation of the center rod *etc*. The contact stress applied to the wire is calculated by dividing the load value by the projected area where the sample and dummy wire overlap (that is calculated by the square of the wire diameter). In a practical situation, the adjacent wires contact each other at some angle θ instead of 90° under the same load. In this situation, the projected area increases by a factor of 1/sin θ, i.e., the contact stress decreases by a factor of sin θ. Furthermore, a GFRP support plate against the Lorentz force is placed. The plate height is slightly larger than the wire radius. To eliminate the generation of electromagnetic forces due to magnetism during the measurement, the setup is constructed with non-magnetic materials such as brass and GFRP.

Measurement procedure is as follows. First, a magnetic field is applied to the sample. Then a load is applied to a given value. Fig. 2 shows a typical example of the applied stress as a function of total displacement. The actual stress value applied to the wire is obtained by subtracting a nearly constant stress offset mainly due to friction during motor drive from the applied stress. During the measurement, the load is constantly

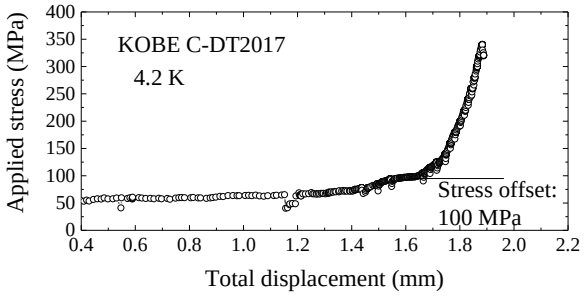

Fig. 2. A typical example of the applied stress as a function of total displacement (Sample: KOBE Cu sheath DT Nb_3Sn strand (C-DT2017)).

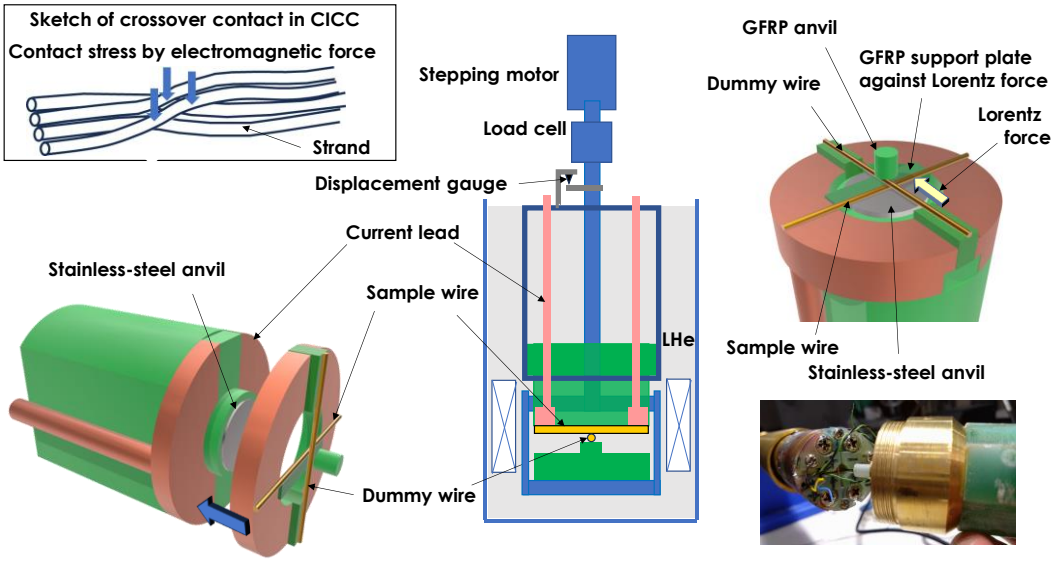

Fig. 1. Sketch of crossover contact in CICC and the setup for I_c measurement simulating crossover contact stress state.

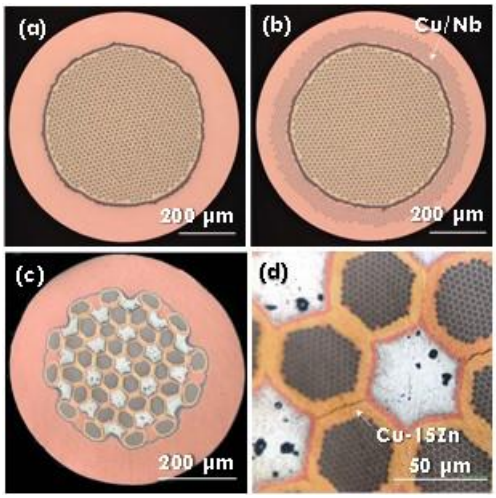

Fig. 3. Cross-sectional optical microscope images of precursor wires (before heat-treatment) for tested Nb_3Sn wires: (a) Furukawa Cu sheath bronze-processed Nb_3Sn strand (LK316), (b) Furukawa CuNb-reinforced bronze-processed Nb_3Sn strand (LK288), (c) Kobe DT Nb_3Sn strand (Cu–15at%Zn matrix, Z-DT2017), and (d) a magnified view of Z-DT2017.

controlled to an indicated value by program control within ±1% error. Subsequently, I_c is measured at given magnetic fields. Then, the load is controlled to a next value and I_c is measured again in magnetic fields. These I_c measurement steps are repeated, when the I_c value degrades drastically.

B. Samples

Fig. 3 shows transverse cross-sections of the tested reinforced Nb_3Sn wires: a normal Cu sheath and a CuNb-reinforced bronze-processed Nb_3Sn wires (developed by Furukawa Electric (LK316, LK288)) [26], and a distributed-tin (DT) configuration Nb_3Sn wires with Cu and a brass (Cu-15at%Zn) matrix (developed by Kobe Steel (C-DT2017, Z-DT2017)) [16]. Table 1 summarized the specifications of the wires.

C. Metallography and EBSD strain analysis

SEM and EBSD were observed by a normal metallographic technique [15]. In EBSD strain analysis, we measured the grain reference orientation deviation (GROD = $\theta_i - \theta_{AVG}$, where θ_i and θ_{AVG} are the orientation of the ith pixel and the average orientation within a grain, respectively). GROD is an index expressing the grain orientation deviation at a given pixel from the average orientation, and a useful index of the qualitative internal strain (residual stress) distribution in the grain due to plastic or elastic deformation [15], [27].

III. Results and Discussion

A. I_c characteristics under crossover contact stress

Fig. 4 plots the voltage (V) vs. current (I) curve for F-Cu-BZ (LK316) at 4.2 K and 14 T. The V–I curves exhibited a small resistive component before a steep voltage increase by a superconducting-normal phase transition. That is presumably due to the effect of current transferring from the electrode to the sample and/or heat generation at the electrodes in the short

TABLE I
Specifications of the Tested Wires

Furukawa bronze-route wire	F-Cu-BZ (LK316)	F-RF2-BZ (LK288)
Wire diameter (mm)	0.825	0.827
Nb filament diameter (μm)	2.3	2.3
Sn diffusion barrier	Ta	Ta
Matrix	Cu–15.7wt%Sn–0.3wt%Ti	Cu–15.7wt%Sn–0.3wt%Ti
Reinforcement	–	Nb-rod-method Cu-20vol%Nb
Cu / CuNb / non-Cu ratio	50 / 0 / 50	27 / 23/ 50

Kobe DT wires	C-DT2017	Z-DT2017
Wire diameter (mm)	0.6	0.6
Nb ratio within barrier (%)	38.6	38.6
Nb filament diameter (μm)	3.4	3.4
Matrix of Nb module	Cu	Cu–15wt%Zn
Matrix of Sn core	Cu	Cu
Nb module diameter (μm)	45	45
Ti ratio within barrier (wt%)	0.7	0.7
Zn ratio within barrier (wt%)	0	5.6
Nb / Sn atomic ratio	2.24	2.24
Cu / non-Cu ratio	1.12	1.12

sample measurement. Here, I_c was defined for Furukawa wires with a criterion of 3 μV/cm and for Kobe wires with 2 μV/cm. The n-index in the equation $V=aI^n$ was determined in the range of 4 to 10 μV. The I_c values of LK316 and LK288 at almost no stress were 166 and 170 A at 14 T (4.2 K) and 142 and 139 A at 15 T (4.2 K), respectively, which were similar to the reported values [26]. Since the KOBE wires showed quench phenomenon at 14 T, I_c measurement was performed at 17 T for KOBE wires. The I_c values of C-DT2017 and Z-DT2017 at zero stress were 59.4 and 66 A at 17 T and 4.2 K, similar to the reported value [16].

Fig. 5 shows normalized I_c vs. contact stress characteristics. As shown in Fig. 5(a) and (b), the reinforced bronze wire exhibited a better stress tolerance. Fig. 6(a) and (b) exhibit the GROD maps on the longitudinal cross-section near the contact point for F-Cu-BZ (LK316) and F-RF2-BZ (LK288), respectively, after loading test. The residual strain spread across the whole region of outer Cu sheath in LK316, whereas in LK288, the high residual strain concentrated predominantly

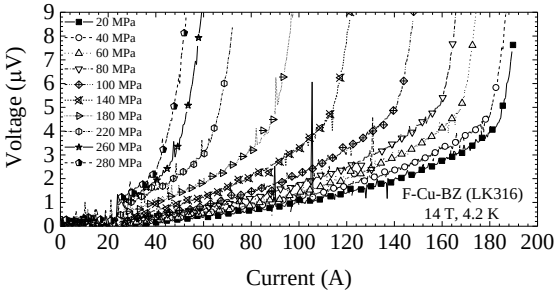

Fig. 4. A typical example of voltage vs. current curves at 14 T and 4.2 K (Sample: Furukawa Cu sheath bronze-processed Nb_3Sn strand (LK316).

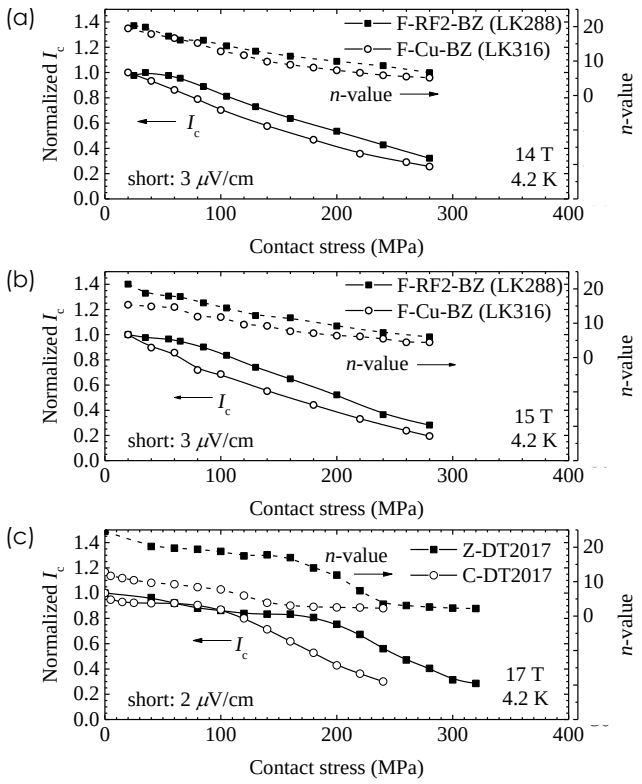

Fig. 5. (a) and (b) Normalized I_c and n-value vs. contact stress for Furukawa bronze-processed Nb_3Sn wires (LK316 and LK288) at 14 and 15 T, 4.2 K, and (c) normalized I_c and n-value vs. contact stress for Kobe C-DT2017 and Z-DT2017 at 17 T, 4.2 K.

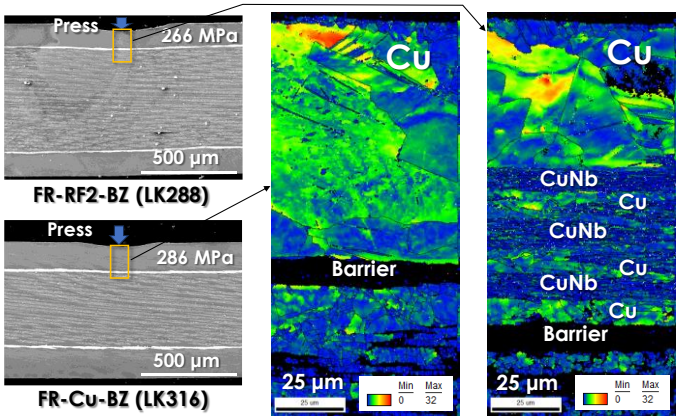

Fig. 6. GROD maps on the longitudinal cross-section of outer sheath for (a) F-Cu-BZ (LK316), (b) F-RF2-BZ (LK288) near the contact point.

at the outermost Cu region but not at the CuNb region. The CuNb reinforcement is expected to be effective in reducing distortion of the internal filament region against contact stress.

Notably, as shown in Fig. 5(c), I_c degradation with respect to contact stress in Z-DT2017 was very small up to approximately 200 MPa. I_c property of the conventional Cu matrix DT strand under contact stress was comparable to that under uniform transverse stress [28]. The excellent transverse stress tolerance of the brass matrix DT strand can be attributed to the advantage of matrix reinforcement to inhibit the

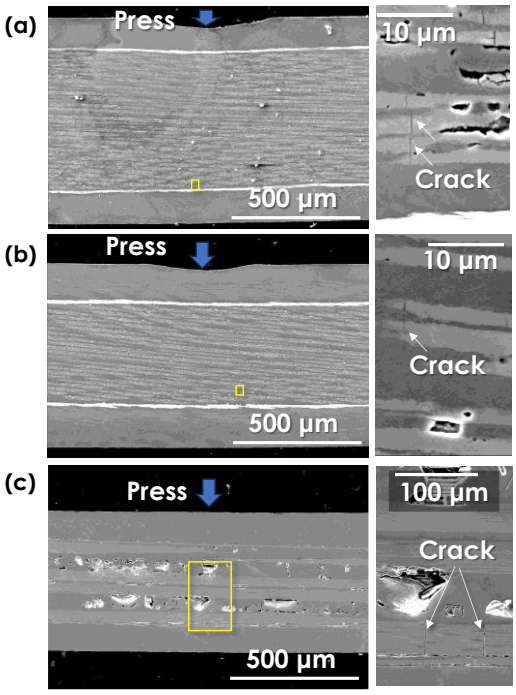

Fig. 7. GROD maps on the longitudinal cross-section near the contact point for (a) F-Cu-BZ (LK316), (b) F-RF2-BZ (LK288), and (c) Z-DT2017 after loading test.

distortion of the filamentary region.

B. Crack observation

A few microcracks were recognized at the opposite side to the contact point in both Furukawa bronze-processed Nb_3Sn wires as shown in Fig. 7(a) and (b). This is similar to the situation where bending strain is applied to the strand. Reportedly, when the wire is subjected to transverse load, cracks tend to form inside the Nb_3Sn filament parallel to the applied transverse load along the longitudinal direction [29], [30]. In such a case, cracks parallel to the longitudinal direction might be difficult to see in the longitudinal cross-section. On the contrast, in Kobe Z-DT2017, large transverse cracks were visible at the opposite side to the contact point. This is presumably due to the mechanical properties of the brass matrix. Generally, in hard matrix multifilamentary wires, once a small crack is initiated, cracks tend to propagate significantly [15], [31].

IV. Conclusion

The stress sensitivity of I_c under crossover contact stress seems to be small, compared with that under uniform transverse stress [19], [22], [23], [26], [32]. The deformation of the Cu sheath by crossover contact is thought to relieve stress concentration to the filamentary region. The reinforcement for the wires was effective to improve the tolerance against transverse stress. Particularly, the DT wire with reinforced matrix exhibited superior tolerance against transverse stress up to approximately 200 MPa. It can be concluded that the use of reinforced Nb_3Sn wires increases the reliability of the TF magnet operation.

REFERENCES

[1] "Joint Special Design Team for Fusion DEMO." [Online]. Available: https://www.fusion.qst.go.jp/rokkasyo/ddjst/l

[2] K. Tobita *et al.*, "Conceptual design of Japan's fusion DEMO reactor (JADEMO) and superconducting coil issues," *J Phys Conf Ser*, vol. 1293, no. 1, p. 012078, Sep. 2019, doi: 10.1088/1742-6596/1293/1/012078.

[3] K. Tobita *et al.*, "Japan's efforts to develop the concept of JA DEMO during the past decade," *Fusion Science and Technology*, vol. 75, no. 5, pp. 372–383, 2019, doi: 10.1080/15361055.2019.1600931.

[4] H. Utoh *et al.*, "Design study of superconducting TF coil concept with rectangular conductor layer winding with high manufacturability and insulation reliability for JA DEMO," *presented at MT-27*, p. WED-OR3-201-03, 2021, [Online]. Available: https://indico.cern.ch/event/975584/contributions/4428241/

[5] H. Utoh, "Magnet design for JA DEMO," *Japan-US Workshop on Fusion Reactor Design and Critical Issues of Fusion Engineering*, 2022, [Online]. Available: https://vltfusion.org/wp-content/uploads/2022/04/Magnet-design-for-JA-DEMO_20220328_HU_v3.pdf

[6] T. Hemmi *et al.*, "Neutron diffraction measurement of internal strain in the first Japanese ITER CS conductor sample," *Supercond Sci Technol*, vol. 26, no. 8, p. 084002, Aug. 2013, doi: 10.1088/0953-2048/26/8/084002.

[7] A. Devred *et al.*, "Challenges and status of ITER conductor production," *Supercond Sci Technol*, vol. 27, no. 4, p. 044001, Apr. 2014, doi: 10.1088/0953-2048/27/4/044001.

[8] V. I. Tronza *et al.*, "Test results of RF ITER TF conductors in the SULTAN test facility," *IEEE Transactions on Applied Superconductivity*, vol. 24, no. 3, p. 4801905, 2014, doi: 10.1109/TASC.2013.2289361.

[9] D. Bessette, "Design of a Nb3Sn cable-in-conduit conductor to withstand the 60 000 electromagnetic cycles of the ITER central solenoid," *IEEE Transactions on Applied Superconductivity*, vol. 24, no. 3, p. 4200505, 2014, doi: 10.1109/TASC.2013.2282399.

[10] Y. Nabara *et al.*, "Impact of cable twist pitch on Tcs-degradation and AC loss in Nb3Sn conductors for ITER central solenoids," *IEEE Transactions on Applied Superconductivity*, vol. 24, no. 3, p. 4200705, 2014, doi: 10.1109/TASC.2013.2284193.

[11] Y. Takahashi *et al.*, "Cabling technology of Nb3Sn conductor for ITER central solenoid," *IEEE Transactions on Applied Superconductivity*, vol. 24, no. 3, p. 4802404, 2014, doi: 10.1109/TASC.2013.2287311.

[12] C. Sanabria, P. J. Lee, W. Starch, A. Devred, and D. C. Larbalestier, "Metallographic autopsies of full-scale ITER prototype cable-in-conduit conductors after full cyclic testing in SULTAN: II. Significant reduction of strand movement and strand damage in short twist pitch CICCs," *Supercond Sci Technol*, vol. 28, no. 12, p. 125003, 2015, doi: 10.1088/0953-2048/28/12/125003.

[13] C. Sanabria, P. J. Lee, W. Starch, A. Devred, and D. C. Larbalestier, "Metallographic autopsies of full-scale ITER prototype cable-in-conduit conductors after full cyclic testing in SULTAN: III. The importance of strand surface roughness in long twist pitch conductors," *Supercond Sci Technol*, vol. 29, no. 7, p. 074002, Jul. 2016, doi: 10.1088/0953-2048/29/7/074002.

[14] "Meeting of the Joint Special Design Team for Fusion DEMO in Japan,"

[15] N. Banno *et al.*, "Metallographic and bending strain property analysis for DEMO candidate Nb_3Sn wires in Japan," *IEEE Transactions on Appiled Superconductivity*, p. submitted, 2023.

[16] N. Banno, T. Morita, T. Yagai, S. Kawashima, and Y. Murakami, "Fundamental study on the effect of Zn addition into Cu matrix in DT method Nb_3Sn conductors," *IEEE Transactions on Applied Superconductivity*, vol. 30, no. 4, p. 6000705, Jun. 2020, doi: 10.1109/TASC.2020.2972209.

[17] M. Sugimoto *et al.*, "Critical current characterization under pure bending strains of prebent Cu-Nb/Nb_3Sn strands for practical react-and-wind process," *IEEE Transactions on Applied Superconductivity*, vol. 26, no. 3, p. 8402205, Apr. 2016, doi: 10.1109/TASC.2016.2529418.

[18] T. Omura, H. Oguro, S. Awaji, K. Watanabe, M. Sugimoto, and H. Tsubouchi, "Effect of Applied Pure Bending Strain on Critical Current for CuNb/Nb3Sn Superconducting Wires," *IEEE Transactions on Applied Superconductivity*, vol. 26, no. 4, p. 8402605, 2016, doi: 10.1109/TASC.2016.2542979.

[19] J. W. Ekin, "Effect of transverse compressive stress on the critical current and upper critical field of Nb_3Sn," *J Appl Phys*, vol. 62, no. 12, pp. 4829–4834, 1987, doi: 10.1063/1.338986.

[20] K. Katagiri *et al.*, "Tensile strain / transverse compressive stress effects in Nb_3Sn multifilamentary wires with CuNb reinforcing stabilizer," in *Advances in Cryogenic Engineering Materials*, L. T. Summers, Ed., Boston, MA: Springer US, 1997, pp. 1423–1432. doi: 10.1007/978-1-4757-9059-7_184.

[21] H. H. J. ten Kate, H. W. Weijers, and J. M. van Oort, "Critical current degradation in Nb_3Sn cables under transverse pressure," *IEEE Transactions on Applied Superconductivity*, vol. 3, no. 1. pp. 1334–1337, 1993. doi: 10.1109/77.233653.

[22] G. Nishijima, K. Watanabe, T. Araya, K. Katagiri, K. Kasaba, and K. Miyoshi, "Effect of transverse compressive stress on internal reinforced Nb $_3$Sn superconducting wires and coils," *Cryogenics (Guildf)*, vol. 45, no. 10–11, pp. 653–658, Oct. 2005, doi: 10.1016/j.cryogenics.2005.08.003.

[23] B. Seeber, A. Ferreira, V. Abächerli, T. Boutboul, L. Oberli, and R. Flükiger, "Transport properties up to 1000 A of Nb_3Sn wires under transverse compressive stress," in *IEEE Transactions on Applied Superconductivity*, Jun. 2007, pp. 2643–2646. doi: 10.1109/TASC.2007.897934.

[24] A. Nijhuis, Y. Ilyin, and W. A. J. Wessel, "Spatial periodic contact stress and critical current of a Nb_3Sn strand measured in TARSIS," *Supercond Sci Technol*, vol. 19, no. 11, pp. 1089–1096, Nov. 2006, doi: 10.1088/0953-2048/19/11/001.

[25] N. Koizumi *et al.*, "Development of large current superconductors using high performance Nb_3Sn strand for ITER," *Physica C: Superconductivity and its Applications*, vol. 463–465, no. SUPPL., pp. 1319–1326, Oct. 2007, doi: 10.1016/j.physc.2007.02.051.

[26] M. Sugimoto *et al.*, "Development of Cu-Nb reinforced Nb_3Sn wires appropriate for large multi-stage stranded cables with short-pitch twisting and low-void ratio," *IEEE Transactions on Applied Superconductivity*, vol. 33, no. 5, Aug. 2023, doi: 10.1109/TASC.2023.3257287.

[27] S. Santra *et al.*, "Insight into the effect of Ti-addition on diffusion-controlled growth and texture of Nb_3Sn intermetallic superconductor phase," *Materialia (Oxf)*, vol. 6, no. January, p. 100276, 2019, doi: 10.1016/j.mtla.2019.100276.

[28] M. Nakamoto *et al.*, "Influence of axial strain and transverse compressive load on critical current of Nb_3Sn wires for the FCC," *IEEE Transactions on Applied Superconductivity*, vol. 33, no. 5, Aug. 2023, doi: 10.1109/TASC.2023.3242919.

[29] T. Bagni, D. Mauro, M. Majkut, A. Rack, and C. Senatore, "Formation and propagation of cracks in RRP Nb_3Sn wires studied by deep learning applied to x-ray tomography," *Supercond Sci Technol*, vol. 35, no. 10, Oct. 2022, doi: 10.1088/1361-6668/ac86ac.

[30] P. Ebermann *et al.*, "Influence of transverse stress exerted at room temperature on the superconducting properties of Nb_3Sn wires," *Supercond Sci Technol*, vol. 32, p. 095010, 2019, doi: 10.1088/1361-6668/ab2e51.

[31] N. Banno, T. Takeuchi, H. Kitaguchi, and K. Tagawa, "Strain tolerance in technical Nb_3Al superconductors," *Supercond Sci Technol*, vol. 19, no. 10, pp. 1057–1062, Oct. 2006, doi: 10.1088/0953-2048/19/10/012.

[32] L. Gämperle, J. Ferradas, C. Barth, B. Bordini, D. Tommasini, and C. Senatore, "Determination of the electromechanical limits of high-performance Nb_3Sn Rutherford cables under transverse stress from a single-wire experiment," *Phys Rev Res*, vol. 2, no. 1, Feb. 2020, doi: 10.1103/PhysRevResearch.2.013211.